Optical Tweezer-Controlled Entanglement Gates with Trapped-Ion Qubits

David Schwerdt,[1,2] Lee Peleg,[1,2] Gal Dekel,[1] Lekshmi Rajagopal,[1] Oz Matoki,[1] Avram Gross,[2] Yotam Shapira,[1,2] Nitzan Akerman,[1] and Roee Ozeri[1,2]
[1]*Department of Physics of Complex Systems, Weizmann Institute of Science, Rehovot 7610001, Israel*
[2]*Quantum Art, Ness Ziona 7403682, Israel*

(Received 11 June 2025; revised 28 October 2025; accepted 8 December 2025; published 15 January 2026)

We propose an entanglement protocol where ions illuminated by optical tweezers serve as control qubits. We experimentally demonstrate this proposal with a controlled Mölmer-Sörensen operation on a three-ion chain, analogous to the canonical Toffoli gate. Our demonstration features cases in which the control qubit was in one of its logical basis states, and not in their superposition, due to dephasing by tweezer beam intensity fluctuations. Finally, we discuss how our protocol generalizes to a broad class of unitary operations and larger qubit systems, enabling a single-pulse implementation of n-controlled unitaries.

DOI: 10.1103/h4c6-463f

Introduction—At the core of any quantum computing (QC) platform is a mechanism for generating entanglement between qubits based upon their shared degrees of freedom. In trapped-ion quantum processors, entanglement is typically mediated by the ions' collective motional modes [1–5]. This approach has yielded high-fidelity entangling gates [6–10], and has motivated efforts to find new ways of interacting with the ions' motional spectrum that optimize gate performance [11–17].

Some methods focus on producing multiqubit entangling gates, which may be highly beneficial in compiling quantum circuits [18–21]. A particularly valuable family of multiqubit operations consists of entangling unitaries that are conditioned on the state of a control qubit, such as the Toffoli gate. These controlled entanglement operations are ubiquitous in quantum algorithms, such as Grover's algorithm [22] or quantum phase estimation [23]. However, they are often challenging to implement efficiently using standard two-qubit gate decompositions or other multiqubit gate methods, which typically result in Ising-type Hamiltonians [19,24–26]. For example, an n-controlled Toffoli gate has been shown to require $\mathcal{O}(n^2)$ CNOT gates [or $\mathcal{O}(n)$ CNOTs when using one or more ancilla qubits]—demanding a substantial overhead in circuit depth [18,27].

In this Letter, we demonstrate a method for realizing controlled unitary operations using a single pulse by leveraging state-dependent optical tweezer potentials. An optical tweezer focused at the position of a trapped ion creates a local confining potential, which modifies the motional mode spectrum. Crucially the effect of the optical tweezer potential depends on the ion's electronic state, enabling qubit-state-dependent shifts in the motional mode frequencies. We use this mechanism as the basis for driving controlled entanglement operations.

The integration of local optical potentials into trapped-ion platforms is an emerging area of interest, with recent theoretical proposals exploring their use for motional mode engineering [28,29], entangling gate implementations [30–32], and scalable quantum computing architectures [31,33,34]. To our knowledge, this Letter presents the first experimental realization of an entangling gate mediated by an optical tweezer in a trapped-ion system.

Controlled entanglement gate—We consider a linear chain of three trapped $^{40}Ca^{+}$ ions, where qubit states are encoded in the ions' $|S_{1/2}, m_J = +1/2\rangle$ and $|D_{5/2}, m_J = +3/2\rangle$ electronic states, denoted correspondingly by $|S\rangle$ and $|D\rangle$. We furthermore consider an ion in the chain that is illuminated by a tightly focused optical tweezer beam, with a wavelength red-detuned near the $S_{\frac{1}{2}} \rightarrow P_{\frac{1}{2}}$ dipole transition.

The optical tweezer generates a dipole potential that corresponds to the induced light shift on the electronic levels. When the ion illuminated by the optical tweezer (hereafter referred to as the tweezed ion) is populated in the $S_{\frac{1}{2}}$ level, it experiences a confining optical potential (o.p.) with frequency [35]

$$\omega_{\mathbf{o.p.}} = 2\sqrt{\frac{\hbar\omega_{\mathbf{LS}}}{m w_0^2}}. \tag{1}$$

Here, $\omega_{\mathbf{LS}}$ denotes the induced light shift, which depends on the optical intensity and the electronic state of the ion, m is the ion's mass, and w_0 is the beam waist. The effect of the optical potential is to increase the energy of each motional mode in accordance with both the intensity of the tweezer beam and the participation of the tweezed ion in the given mode.

Here we are primarily interested in the low intensity regime, where the strength of the optical potential is far below that of the rf electronic trap. In this regime, the shift of a given motional mode frequency, which we denote as $\Delta\nu_m$ for mode index m, is typically linear with the applied

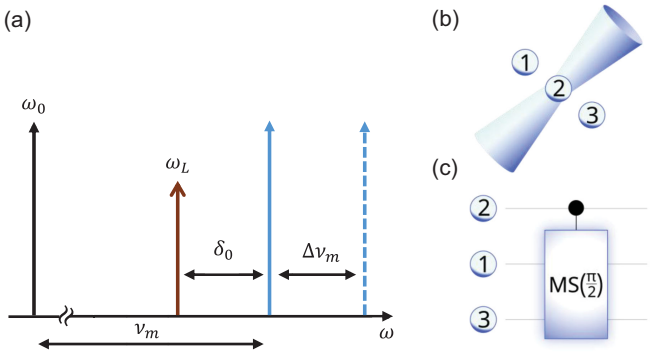

FIG. 1. (a) Spectral picture for the optical tweezer-controlled entanglement gate. Following the Mølmer-Sørensen (MS) protocol, the gate drive laser (red) is detuned by δ_0 from the natural mode frequency (solid blue). The detuning from the shifted mode frequency (dashed blue) is then $\delta_0 + \Delta\nu_m$. The motional mode shift occurs only when the tweezed ion is in the $|S\rangle$ state. (b) Schematic of the physical implementation, where the central ion (qubit 2) is illuminated by an optical tweezer and the outer ions (qubits 2 and 3) undergo MS dynamics. (c) Setting $\Delta\nu_m = \delta_0$ yields a controlled fully entangling MS gate.

optical intensity. A derivation of the ions' motional mode frequencies and vectors in the presence of optical potentials is given in Supplemental Material (SM) [36].

By contrast to the ground state, the induced light shift on the $D_{\frac{5}{2}}$ manifold is negligible. Correspondingly, when the ion is populated in the $|D\rangle$ state, it does not experience an optical potential and the motional modes are unaffected. In this way, the motional spectrum of the trapped-ion chain is dependent on the qubit state of the tweezed ion.

To drive the gate we make use of the well-known Mølmer-Sørensen (MS) protocol [2,3]. The MS gate is generated by driving the qubits with a global bichromatic laser field, containing the two frequencies, $\omega_{\mathrm{L},\pm} = \omega_0 \pm (\nu_m + \delta)$, where ω_0 is the qubits' transition frequency, ν_m the frequency of the mth motional mode of the trap, and δ is the gate detuning. The strength of the driving field is given by the Rabi frequency, Ω. The gate is operated in the adiabatic regime, $\delta \ll \nu$, such that all other modes of motion remain decoupled. This drive acts to generate a spin-dependent force that mediates interactions between the qubits. For a gate duration, $\tau_{\mathrm{g}} = 2\pi/\delta$, the qubit and motional degrees of freedom decouple, and the qubits undergo a correlated $\sigma_x \otimes \sigma_x$ (denoted as XX) rotation with an entanglement phase, $\Phi \propto (\Omega^2/\delta)\tau_g$.

Combining this with our mechanism for a qubit-state dependent motional shift, we design an entangling gate that is controlled by the state of the tweezed ion. Specifically, the gate detuning depends on the motional shift, $\delta = \delta_0 + \Delta\nu_m$, where δ_0 is the value of the detuning in absence of a motional shift. If the tweezed ion qubit is in the $|D\rangle$ state we have $\delta = \delta_0$; whereas if it is in $|S\rangle$ state then $\delta = \delta_0 + \Delta\nu_m$. The relevant frequencies describing the gate drive are illustrated schematically in Fig. 1(a) (depicted here for the blue sideband and following symmetrically for the red sideband).

We assume that the light shift on the tweezed ion is far larger than the Rabi frequency of the driving field ($\omega_{\mathbf{LS}} \gg \Omega$). Therefore, regardless of its quantum state, the tweezed ion itself does not participate in the gate dynamics as the driving field, $\omega_{\mathrm{L},\pm}$, is far off resonant with its light-shifted $S_{\frac{1}{2}} \to D_{\frac{5}{2}}$ transition frequency. Finally, we consider the layout of Fig. 1(b) where the central ion (corresponding to qubit 2) is tweezed. The nontweezed ions (corresponding to qubits 1 and 3) participate equally in the chosen motional mode, as will be the case in the demonstration discussed below.

The dynamics of the nontweezed ions follow the MS unitary evolution [3], such that at integer multiples of the gate time, $T = n\tau_{\mathrm{g}}$, qubits 1 and 3 evolve with the unitary operator $U_{1,3} = e^{i\Phi_m J_x^2}$, where $J_x = [(X_1 + X_2)/2]$, and the entanglement phase is expressed as

$$\Phi_m = \frac{\eta_m^2 \Omega^2 T}{\delta}, \tag{2}$$

with η_m the Lamb-Dicke (LD) parameter associated with the mth mode of motion and Ω the Rabi frequency of the gate drive.

Clearly, the unitary dynamics can be modified by tuning the value of δ via the motional shift. As an example for the utility of this protocol, we consider the special case where the motional shift is configured to exactly equal the detuning from the natural mode frequency $\Delta\nu_m = \delta_0$. Then choosing a gate time of $T = 2\tau_{\mathrm{g}} = (4\pi/\delta_0)$ and setting the Rabi frequency as $\Omega = (\delta_0/2\eta_m)$, the entanglement phase is given by

$$\Phi_m = \begin{cases} \pi, & \text{if ion 2 in } |D\rangle \\ \frac{\pi}{2}, & \text{if ion 2 in } |S\rangle \end{cases}. \tag{3}$$

Equation (3) shows that if the tweezed ion is in the $|D\rangle$ state, the gate drive simply results in a bit-flip of qubits 1 and 3, i.e., $U_{1,3} \mapsto e^{i\pi J_x^2} = X_1 X_3$; whereas if the tweezed ion is in the $|S\rangle$ state, the result is a fully entangling unitary, $U_{1,3} \mapsto e^{i(\pi/2)J_x^2} = (1/\sqrt{2})(I + iX_1X_3)$. At this point it is possible to perform an additional X rotation on qubits 1 and 3, resulting in the controlled-MS (CMS) gate, represented in circuit notation in Fig. 1(c):

$$U_{\mathbf{CMS}} = e^{-i\frac{\pi}{8}(I_2 - Z_2)X_1X_3}. \tag{4}$$

Evidently, this protocol enables controlled fully-entangling operations, analogous to the controlled-CNOT (i.e. Toffoli) gate.

Gate implementation—We demonstrated the controlled entanglement protocol described above in a chain of three ions. The central ion is illuminated by an optical tweezer with a nearly Gaussian beam profile and a waist of

$w_0 \approx 1$ μm. The wavelength of the optical tweezer is 400 nm, detuned from the ions' $S_{\frac{1}{2}} \rightarrow P_{\frac{1}{2}}$ dipole transition at 397 nm. Low-intensity individual addressing beams (at 400 nm) on the outer ions are used for light-shift crosstalk compensation and state initialization. Further details of these protocols, as well as of the experimental system, are provided in SM [36].

The gate driving field, controlling the ions' $S_{\frac{1}{2}} \leftrightarrow D_{\frac{5}{2}}$ transition, is a narrow linewidth laser at 729 nm. It propagates along the trap axis as a global beam, delivering nearly uniform intensity to all ions. The axial center-of-mass (c.m.) mode frequency is set to $\nu_1 = (2\pi)\,360$ kHz, with higher modes at $\nu_2 = (2\pi)\,624$ kHz, and $\nu_3 = (2\pi)\,866$ kHz respectively. The gate is driven on the third (i.e., zig-zag) mode due to its low heating rate (<1 quanta per second) and high participation of the central ion. We use relatively low axial trap frequencies to keep the ions well separated and to allow for modest light shifts to produce a large effect, though this comes at the cost of elevated heating rates.

A crucial parameter is the value of the motional frequency shift, which sets the gate time and is tunable via the power in the optical tweezer beam. We generated a motional shift of $(2\pi)\,4.0(1)$ kHz, corresponding to a gate time of $T = 500$ μs, and resulting in a light shift of $(2\pi)\,10.4(2)$ MHz on the tweezed ion (requiring roughly 1 mW of input optical power).

The main experimental challenge caused by the large light shift is maintaining the phase of the optical qubit encoded in the tweezed ion. Intensity fluctuations of the optical tweezer beam result in Pauli-Z noise on the control qubit causing its quantum state to dephase faster than the timescale of the gate. We note that such fluctuations also produce motional frequency noise; however, this effect is much weaker than qubit dephasing.

We observed intensity noise on the optical tweezer (dominated by beam pointing fluctuations) at the 1%–10% level. This implies a qubit dephasing noise amplitude of up to ∼1 MHz—over 2 orders of magnitude faster than the gate. Because of this strong dephasing channel, we limit our current experiment to cases where the control qubit ion is initialized in one of the basis states. Ultimately in order for the gate to be practical, it must preserve an arbitrary superposition of the control qubit. Several routes exist to overcome this limitation: technical improvements to the optical system can strongly suppress beam-pointing fluctuations, while active error-suppression strategies such as dynamical decoupling can be incorporated into the gate sequence. Furthermore the control qubit can be encoded in a decoherence-free subspace that is resilient to global light shift noise resulting from common beam intensity fluctuations. These approaches suggest a clear path toward realizing a fully coherent version of the gate protocol; we discuss them in greater detail in SM [36]. Nevertheless, our present result demonstrates the validity of using qubit-state-dependent motional shifts to implement controlled entanglement operations.

Results and analysis—We run our gate protocol with two different initial states, which we label cases "*D*" and "*S*," respectively: $|\psi_D(0)\rangle = |SDS\rangle$ and $|\psi_S(0)\rangle = |SSS\rangle$. We aim to see that the state of the central ion influences the gate dynamics; in particular, when the central ion is in the $|S\rangle$ state, the gate detuning should effectively double. At the gate time, T, the state of the outer ions in each case should be $|\psi_D(T)\rangle = |DD\rangle$ and $|\psi_S(T)\rangle = (1/\sqrt{2})(|SS\rangle + i|DD\rangle)$. As mentioned above, in either case the state of the central ion is unaffected by the gate as its qubit frequency is far off resonant with the driving field.

The measured gate dynamics for both choices of initial state, as well as a fit to a numerical simulation, are shown in Fig. 2. The gate detuning extracted from the fit in each case is $\delta_D = (2\pi)\,4.05(2)$ kHz and $\delta_S = (2\pi)\,8.20(5)$ kHz, respectively, thus verifying that the optical potential affects the gate dynamics in the expected way. The state fidelities in case D and S are measured, respectively, to be $\mathcal{F}_{\mathcal{D}} = 93.5(9)\%$ and $\mathcal{F}_{\mathcal{S}} = 85(1)\%$. Consistent with standard practice for characterizing MS gates [42], fidelities are extracted from measurements starting in the $|SS\rangle$ state through analysis of populations and, in case S, the contrast of a parity measurement following the gate (see SM [36]).

The observed fidelities are limited by technical noise sources—primarily fluctuations in the gate-drive laser intensity, trap-frequency noise, high initial temperature of the axial c.m. mode, and errors in the motional shift (case S). Further discussion of the impact of these effects on gate fidelity is provided in SM [36]. Importantly, comparable performance to the gate of case D is obtained using a standard MS gate without the optical tweezer for the same gate time and trap frequency—suggesting that the presence of the optical tweezer itself does not significantly impact gate fidelity.

Generalizing the method—We note that our method can be generalized to produce a larger family of conditional unitary operations. This is done by adding degrees of freedom to control the pulse shape of the gate driving field. For example, instead of applying a bichromatic field as in the MS protocol, we may apply several laser tones as is typically done for multimode entanglement gates [16]. In that scheme, multiple laser tones are applied within the range of motional mode frequencies of the ion chain. By varying the amplitude in each tone, one can control the entanglement phase accumulated in each motional mode and thereby implement a variety of XX-type unitaries.

In our case of a three-ion chain, we consider an effective two-mode system described by the natural and shifted mode frequencies. While both describe the same vibrational mode, we may treat this analogously to a multimode problem (see also Ref. [32]). Multiple laser tones would be interspersed around both frequencies—allowing us to control the entanglement phase accumulated in each mode. One possible choice is to find a gate drive spectrum that

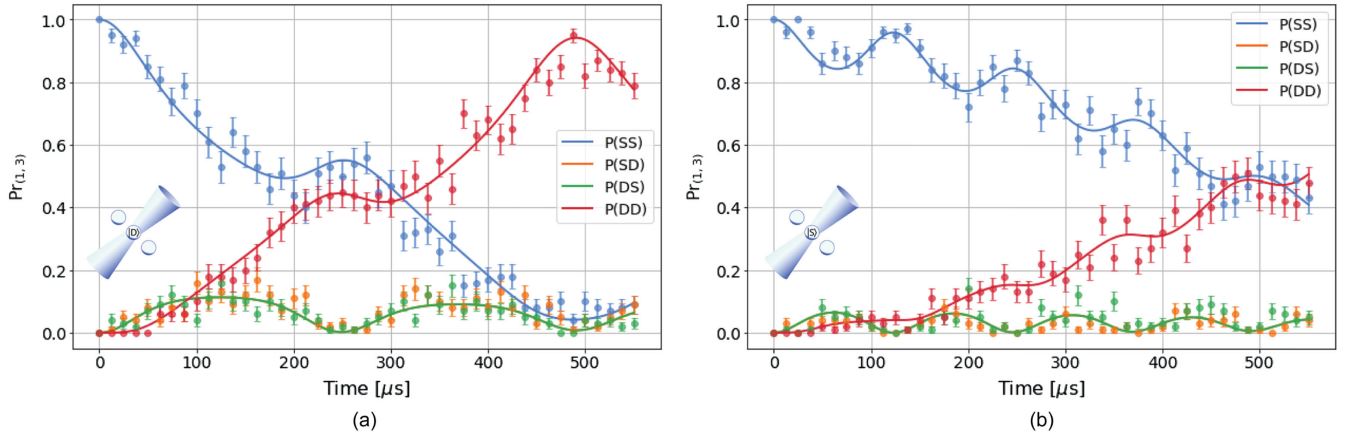

FIG. 2. Gate dynamics for the outer ions in a three-ion chain, controlled by the qubit state of the central ion that is illuminated by an optical tweezer. Shown here are two gates driven with the same laser detuning $\delta_0 = (2\pi)\,4$ kHz and Rabi frequency $\Omega = (\delta_0/2\eta_m) = (2\pi)\,47.4$ kHz, but two different choices of initial state: (a) $|\psi_A(0)\rangle = |SDS\rangle$ and (b) $|\psi_B(0)\rangle = |SSS\rangle$. The motional frequency shift due to the optical tweezer potential is tuned to match the gate detuning, 4 kHz. When the central ion is in $|S\rangle$ state, the effective detuning doubles resulting in qualitatively different dynamics. At the gate time $T = (4\pi/\delta_0)$, the gate results in either (a) the nonentangling unitary $U_{1,3} = X_1X_3$, or (b) the fully entangling unitary $U_{1,3} = (1/\sqrt{2})(I + iX_1X_3)$.

enforces zero phase in the unshifted mode, realizing the identity operator, and an arbitrary value in the shifted mode. This produces a controlled-MS unitary with arbitrary angle [generalized from the case of $\Phi = (\pi/2)$ discussed above].

In addition to enabling a wide variety of unitary operations for the three-ion case, our gate protocol can also be extended to larger qubit systems. Specifically the gate can be generalized to a chain of $n + 2$ ions where n of those ions are illuminated by optical tweezers. Here we assume this gate is performed on the c.m. mode such that each ion participates equally in the motional mode. To a very good approximation (for low optical tweezer intensities considered here), the total c.m. mode frequency shift depends solely on the number of tweezed ions in the $|S\rangle$ state—not on their index within the chain. We therefore get $n + 1$ different mode configurations. Coupling to other non-c.m. modes of the ion chain can be neglected; for a harmonic axial potential, the next-highest-frequency mode is a factor of $\sqrt{3}$ higher than the c.m. regardless of n. We note that this approach requires low axial heating rates; alternatively, one could consider working with the radial c.m. mode.

Following the same logic as for the multimode gates mentioned above, one could enforce zero entanglement phase in each effective mode aside from one (e.g., the last mode corresponding to all tweezed ions in $|S\rangle$) which receives a phase of $(\pi/2)$. This results in an n-controlled MS gate, depicted in circuit notation in Fig. 3(a). We simulate this operation (optimally realizing the desired

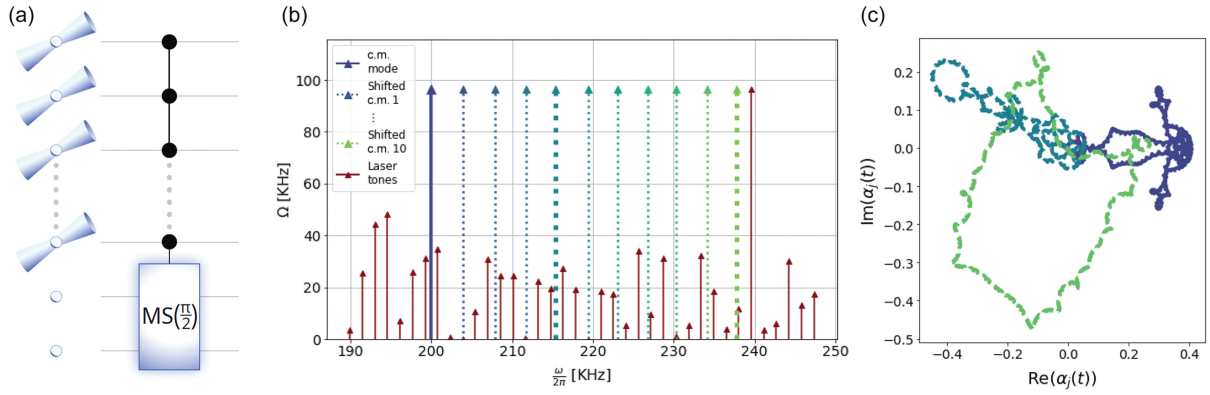

FIG. 3. Extension of the optical tweezer-controlled gate method to larger qubits systems. (a) Circuit diagram for an n-controlled MS gate. (b) Calculated drive spectrum to implement the gate in (a), involving $n = 10$ ions illuminated by optical tweezers as well as 2 nontweezed ions. The gate drive tones (red) straddle an effective mode spectrum, which contains the natural c.m. mode and n shifted frequencies (blue solid and dashed colored lines respectively). The natural c.m. mode (dark blue), as well as the fourth and tenth shifted modes (teal and green respectively), are highlighted. (c) Phase space trajectories of the highlighted modes (for the $|SS\rangle$ state of the two target qubits).

entanglement while also imposing phase-space closure according to the procedure of [16]) for $n = 10$ using realistic experimental parameters, and show the resulting gate drive spectrum in Fig. 3(b). Here the solid blue and dashed colored lines correspond, respectively, to the natural c.m. frequency and each possible shifted mode frequency. The red lines correspond to tones of the laser drive, and their height denotes the Rabi frequency (i.e., laser power) associated with each tone. The phase-space trajectories $\alpha_j(t)$ of three highlighted modes during the gate (see SM [36]) are shown in Fig. 3(c). Trajectories of each mode, as well as their respective displacements over time, are shown in SM [36].

In this calculated example, the gate time is 644 μs—comparable to the demonstrated three-ion case. The total Rabi frequency required for the gate is $\Omega = (2\pi)\,120$ kHz; as is the case for MS, the Rabi frequency is expected to scale as the square root of the chain size. The required optical tweezer intensity, in order to achieve the same motional shift, also increases with chain size. In this case, a 4 kHz shift per tweezed ion requires a $(2\pi)\,20$ MHz light shift.

Notably the gate time in this method does not scale with n. In fact, the minimum gate time in the multimode case corresponds to the frequency splitting between the different shifted modes [17]; therefore, in our case, the gate time would scale inversely with the frequency shift $T \sim (1/\Delta\nu_m)$ regardless of the number of ions. Furthermore (as mentioned above and described in SM [36]), dynamical decoupling pulses can be straightforwardly incorporated into the gate to mitigate the effects of optical tweezer intensity noise. The required number of such pulses per control qubit depends only on the noise spectrum and does not scale with n. Since these pulses are fast and can be applied in parallel to all control qubits, the relative overhead compared to the entangling gate time remains minimal.

The n-controlled MS operator discussed here is equivalent (up to single qubit rotations) to an $(n-1)$-controlled Toffoli gate, and requires only a single driving pulse.

Conclusion and outlook—We have described and demonstrated a protocol for controlled entanglement operations, making use of state-dependent optical tweezer potentials on trapped-ion qubits. We have shown how the protocol can naturally be extended to drive multiply-controlled unitaries, with a gate time that is independent of system size. In particular, this enables an efficient implementation of multiply-controlled Toffoli gates, which could be highly useful in many quantum computing applications.

Acknowledgments—We thank Jonathan Nemirovsky for helpful discussions.

Data availability—The data that support the findings of this article are not publicly available. The data are available from the authors upon reasonable request.

[1] J. I. Cirac and P. Zoller, Quantum computations with cold trapped ions, Phys. Rev. Lett. **74**, 4091 (1995).
[2] A. Sørensen and K. Mølmer, Quantum computation with ions in thermal motion, Phys. Rev. Lett. **82**, 1971 (1999).
[3] A. Sørensen and K. Mølmer, Entanglement and quantum computation with ions in thermal motion, Phys. Rev. A **62**, 022311 (2000).
[4] D. Leibfried, B. DeMarco, V. Meyer, D. Lucas, M. Barrett, J. Britton, W. M. Itano, B. Jelenković, C. Langer, T. Rosenband, and D. J. Wineland, Experimental demonstration of a robust, high-fidelity geometric two ion-qubit phase gate, Nature (London) **422**, 412 (2003).
[5] C. Ospelkaus, C. E. Langer, J. M. Amini, K. R. Brown, D. Leibfried, and D. J. Wineland, Trapped-ion quantum logic gates based on oscillating magnetic fields, Phys. Rev. Lett. **101**, 090502 (2008).
[6] C. J. Ballance, T. P. Harty, N. M. Linke, M. A. Sepiol, and D. M. Lucas, High-fidelity quantum logic gates using trapped-ion hyperfine qubits, Phys. Rev. Lett. **117**, 060504 (2016).
[7] J. P. Gaebler, T. R. Tan, Y. Lin, Y. Wan, R. Bowler, A. C. Keith, S. Glancy, K. Coakley, E. Knill, D. Leibfried, and D. J. Wineland, High-fidelity universal gate set for $^{9}Be^{+}$ ion qubits, Phys. Rev. Lett. **117**, 060505 (2016).
[8] T. P. Harty, M. A. Sepiol, D. T. C. Allcock, C. J. Ballance, J. E. Tarlton, and D. M. Lucas, High-fidelity trapped-ion quantum logic using near-field microwaves, Phys. Rev. Lett. **117**, 140501 (2016).
[9] C. M. Löschnauer, J. M. Toba, A. C. Hughes, S. A. King, M. A. Weber, R. Srinivas, R. Matt, R. Nourshargh, D. T. C. Allcock, C. J. Ballance, C. Matthiesen, M. Malinowski, and T. P. Harty, Scalable, high-fidelity all-electronic control of trapped-ion qubits, PRX Quantum **6**, 040313 (2025).
[10] S. Moses *et al.*, A race-track trapped-ion quantum processor, Phys. Rev. X **13**, 041052 (2023).
[11] Y. Shapira, R. Shaniv, T. Manovitz, N. Akerman, and R. Ozeri, Robust entanglement gates for trapped-ion qubits, Phys. Rev. Lett. **121**, 180502 (2018).
[12] P. H. Leung, K. A. Landsman, C. Figgatt, N. M. Linke, C. Monroe, and K. R. Brown, Robust 2-qubit gates in a linear ion crystal using a frequency-modulated driving force, Phys. Rev. Lett. **120**, 020501 (2018).
[13] C. H. Valahu, I. Apostolatos, S. Weidt, and W. K. Hensinger, Quantum control methods for robust entanglement of trapped ions, J. Phys. B **55**, 204003 (2022).
[14] Y. Shapira, S. Cohen, N. Akerman, A. Stern, and R. Ozeri, Robust two-qubit gates for trapped ions using spin-dependent squeezing, Phys. Rev. Lett. **130**, 030602 (2023).
[15] N. Grzesiak, R. Blümel, K. Wright, K. M. Beck, N. C. Pisenti, M. Li, V. Chaplin, J. M. Amini, S. Debnath, J.-S. Chen, and Y. Nam, Efficient arbitrary simultaneously entangling gates on a trapped-ion quantum computer, Nat. Commun. **11**, 2963 (2020).
[16] Y. Shapira, R. Shaniv, T. Manovitz, N. Akerman, L. Peleg, L. Gazit, R. Ozeri, and A. Stern, Theory of robust multiqubit nonadiabatic gates for trapped ions, Phys. Rev. A **101**, 032330 (2020).
[17] Y. Shapira, L. Peleg, D. Schwerdt, J. Nemirovsky, N. Akerman, A. Stern, A. B. Kish, and R. Ozeri, Fast design

and scaling of multi-qubit gates in large-scale trapped-ion quantum computers, arXiv:2307.09566.
[18] D. Maslov and Y. Nam, Use of global interactions in efficient quantum circuit constructions, New J. Phys. **20**, 033018 (2018).
[19] S. Bravyi, D. Maslov, and Y. Nam, Constant-cost implementations of clifford operations and multiply-controlled gates using global interactions, Phys. Rev. Lett. **129**, 230501 (2022).
[20] J. Nemirovsky, M. Chuchem, and Y. Shapira, Efficient compilation of quantum circuits using multi-qubit gates, arXiv:2501.17246.
[21] D. Schwerdt, Y. Shapira, T. Manovitz, and R. Ozeri, Comparing two-qubit and multiqubit gates within the toric code, Phys. Rev. A **105**, 022612 (2022).
[22] L. K. Grover, A fast quantum mechanical algorithm for database search, in *Proceedings of the 28th Annual ACM Symposium on Theory of Computing (STOC)* (1996), pp. 212–219, arXiv:quant-ph/9605043.
[23] A. Y. Kitaev, Quantum measurements and the Abelian stabilizer problem, arXiv:quant-ph/9511026.
[24] J. M. Martyn, Z. M. Rossi, A. K. Tan, and I. L. Chuang, Grand unification of quantum algorithms, PRX Quantum **2**, 040203 (2021).
[25] A. Gilyén, Y. Su, G. H. Low, and N. Wiebe, Quantum singular value transformation and beyond: Exponential improvements for quantum matrix arithmetics, in *Proceedings of the 51st Annual ACM SIGACT Symposium on Theory of Computing, STOC '19* (ACM, New York, NY, USA, 2019), pp. 193–204.
[26] S. S. Ivanov, P. A. Ivanov, and N. V. Vitanov, Efficient construction of three- and four-qubit quantum gates by global entangling gates, Phys. Rev. A **91**, 032311 (2015).
[27] A. Barenco, C. H. Bennett, R. Cleve, D. P. DiVincenzo, N. Margolus, P. Shor, T. Sleator, J. A. Smolin, and H. Weinfurter, Elementary gates for quantum computation, Phys. Rev. A **52**, 3457 (1995).
[28] Y. H. Teoh, M. Sajjan, Z. Sun, F. Rajabi, and R. Islam, Manipulating phonons of a trapped-ion system using optical tweezers, Phys. Rev. A **104**, 022420 (2021).
[29] A. R. Vasquez, C. Mordini, D. Kienzler, and J. Home, State-dependent control of the motional modes of trapped ions using an integrated optical lattice, arXiv:2411.03301.
[30] M. Mazzanti, R. Gerritsma, R. J. C. Spreeuw, and A. Safavi-Naini, Trapped ions quantum logic gate with optical tweezers and the magnus effect, Phys. Rev. Res. **5**, 033036 (2023).
[31] M. Mazzanti, R. X. Schüssler, J. D. Arias Espinoza, Z. Wu, R. Gerritsma, and A. Safavi-Naini, Trapped ion quantum computing using optical tweezers and electric fields, Phys. Rev. Lett. **127**, 260502 (2021).
[32] C. Robalo Pereira, L. J. Bond, M. Mazzanti, R. Gerritsma, and A. Safavi-Naini, Fast quantum gates with electric field pulses and optical tweezers in trapped ions, Entropy **27**, 595 (2025).
[33] T. Olsacher, L. Postler, P. Schindler, T. Monz, P. Zoller, and L. M. Sieberer, Scalable and parallel tweezer gates for quantum computing with long ion strings, PRX Quantum **1**, 020316 (2020).
[34] D. Schwerdt, L. Peleg, Y. Shapira, N. Priel, Y. Florshaim, A. Gross, A. Zalic, G. Afek, N. Akerman, A. Stern, A. B. Kish, and R. Ozeri, Scalable architecture for trapped-ion quantum computing using RF traps and dynamic optical potentials, Phys. Rev. X **14**, 041017 (2024).
[35] R. Grimm, M. Weidemüller, and Y. B. Ovchinnikov, *Optical Dipole Traps for Neutral Atoms* (Academic Press, New York, 2000), pp. 95–170.
[36] See Supplemental Material at http://link.aps.org/supplemental/10.1103/h4c6-463f for further details, which includes Refs. [37–41].
[37] D. James, Quantum dynamics of cold trapped ions with application to quantum computation, Appl. Phys. B **66**, 181 (1998).
[38] X. Mai, L. Zhang, Q. Yu, J. Zhang, and Y. Lu, Scalable entangling gates on ion qubits via structured light addressing, arXiv:2506.19535.
[39] S. Saner, O. Băzăvan, M. Minder, P. Drmota, D. J. Webb, G. Araneda, R. Srinivas, D. M. Lucas, and C. J. Ballance, Breaking the entangling gate speed limit for trapped-ion qubits using a phase-stable standing wave, Phys. Rev. Lett. **131**, 220601 (2023).
[40] M. J. Biercuk, H. Uys, A. P. VanDevender, N. Shiga, W. M. Itano, and J. J. Bollinger, Optimized dynamical decoupling in a model quantum memory, Nature (London) **458**, 996 (2009).
[41] K. D. Petersson, J. R. Petta, H. Lu, and A. C. Gossard, Quantum coherence in a one-electron semiconductor charge qubit, Phys. Rev. Lett. **105**, 246804 (2010).
[42] J. Benhelm, G. Kirchmair, C. F. Roos, and R. Blatt, Towards fault-tolerant quantum computing with trapped ions, Nat. Phys. **4**, 463 (2008).